PHILOSOPHICAL TRANSACTIONS OF THE ROYAL SOCIETY A MATHEMATICAL, PHYSICAL & ENGINEERING SCIENCES

Satellite-Borne Measurements of Middle-Atmosphere Composition [and Discussion]

J. M. Russell, M. P. McCormick, D. G. Andrews and F. W. Taylor

Phil. Trans. R. Soc. Lond. A 1987 **323**, 545-565
doi: 10.1098/rsta.1987.0104

Phil. Trans. R. Soc. Lond. A **323**, 545–565 (1987)
Printed in Great Britain

Satellite-borne measurements of middle-atmosphere composition

By J. M. Russell III and M. P. McCormick
Atmospheric Sciences Division, NASA Langley Research Center, Hampton, Virginia 23665-5225, *U.S.A.*

A number of satellite experiments have been launched in recent years with the goal of providing fundamental data needed for analysis of photochemistry, radiation, dynamics, and transport processes. Collectively, these experiments have accumulated information on the vertical and horizontal distributions of a host of minor constituents in the middle atmosphere. The combined satellite data set includes new global measurements of O_3, NO_2, N_2O, HNO_3, CH_4, H_2O, and aerosols, and more-limited data on CO, N_2O_5, $ClONO_2$, HNO_4, COF_2, and CH_3Cl. These data have provided descriptions of (1) the geographic extent and year-to-year change in the recently discovered Antarctic ozone hole; (2) interannual variability in N_2O and CH_4; (3) the winter high latitude NO_2 'cliff'; (4) exchange of NO_2 from the mesosphere to the stratosphere during polar night; (5) a lower limit total odd nitrogen distribution that displays a maximum that exceeds model calculated values; (6) variations in the newly discovered polar stratospheric clouds (PSCs) seen in the north and south polar regions; and (7) details of latitudinal and temporal aerosol variability. The existing satellite data set is deficient in certain key measurements including OH, HO_2, H_2O_2, polar night N_2O_5, radiatively important aerosol properties, and simultaneous measurements of aerosols and gases involved in heterogeneous processes.

Introduction

Considerable attention has been focused on the middle atmosphere in recent years because of concerns that anthropogenic activity can alter the natural composition of the region and lead to depletion of total ozone. Stimulated by these concerns, many measurements have been made of middle-atmosphere composition and structure from ground-based, balloon, rocket, and satellite platforms. Also, extensive data analyses and atmospheric studies have been conducted by using one-dimensional and multi-dimensional models (see, for example, Solomon *et al.* 1985*a*; Grose *et al.* 1985; Callis *et al.* 1986).

The chemical focus of these studies has centred around three main families that can cause catalytic ozone destruction. These include oxides of nitrogen (NO_x), oxides of chlorine (ClO_x), and oxides of hydrogen (HO_x). A principal worry has been the effect of chlorofluorocarbons (CFCs) on ozone, and a number of results have been reported on this subject (see, for example, National Academy of Sciences 1984; NASA/World Meteorological Organization (WMO) 1986). Concerns have been heightened in the past two years with the discovery by Farman *et al.* (1985) of a deep total ozone minimum that has occurred annually since the mid-1960s in September and October over Halley Bay (75.5° S, 26.8° W). The depth of the minimum has become progressively greater, reaching values as low as 30–40% of the levels that exist for the long-term climatological average for these months. Later in the year, for example November, the ozone returns to near normal values. Numerous theories focusing on this phenomenon have been developed and described in the literature (see Solomon *et al.*

1986*a*; McElroy *et al.* 1986; Tung *et al.* 1986; Callis & Natarajan 1986). Since the Farman *et al.* (1985) paper, further evidence of the ozone hole has come forth from a reanalysis of data collected from the solar backscatter ultraviolet (SBUV) and total ozone mapping spectrometer (TOMS) experiments on the *Nimbus* 7 satellite (Krueger *et al.* 1985).

The Antarctic ozone hole is just one of several atmospheric phenomena whose geographic and temporal characteristics have now been elucidated with satellite observations. Flights of the Solar Mesosphere Explorer (SME) (Barth *et al.* 1983), SBUV (McPeters *et al.* 1984), TOMS (Heath *et al.* 1978), the stratospheric and mesospheric sounder (SAMS) (Jones & Pyle 1984), the limb infrared monitor of the stratosphere (LIMS) (Gille & Russell 1984), the stratospheric aerosol and gas experiment (SAGE) (McCormick *et al.* 1979), and SAGE II (McMaster 1986) have collectively provided data on vertical profiles and geographic distributions of temperature, O_3, NO_2, N_2O, HNO_3, H_2O, CH_4, CO, and aerosols. In addition, two other experiments launched on shuttle, the Spacelab 1 grille spectrometer (Lippens *et al.* 1984) and the Spacelab 3 atmospheric trace molecule spectroscopy (ATMOS) experiment (Farmer & Raper 1986), conducted solar-occultation measurements of a host of minor gases on 1 and 2 December 1983, and 30 April–1 May 1985, respectively. The grille spectrometer collected data at 33° N and 68° S, and ATMOS made measurements at 30° N and 47° S. Even though space and time coverage was limited, data from these experiments extended well into the mesosphere, which is a region that has only been probed extensively by SME and in that case only for O_3. Direct global-scale measurements of odd chlorine (ClO_x) and odd hydrogen (HO_x) species have not been possible up to now.

A summary of monthly mean temperature and composition data collected by satellites was presented by Russell *et al.* (1986). In that paper, the authors compare results from various middle atmosphere experiments, they discuss data limitations and quality, and they show both zonal-mean and polar-stereographic distributions as a first step in deriving a 'climatology' for middle-atmosphere composition. The intent of this paper is to present and discuss available composition measurements. Geographic distributions will be described with emphasis on those features that are not currently reproduced well by model calculations.

Composition measurements

An extensive discussion of composition measurements made from satellites, an overview of key questions the data have raised, and a summary of geophysical implications of the results were presented in the NASA/WMO (1986) report. Some of this information will be included in this paper for completeness. In addition, new results developed since NASA/WMO (1986) and areas not stressed in the report will be emphasized. The discussion will be organized according to molecule and focused on remaining questions suggested by the data and salient features of the geographic distributions.

Ozone (O_3)

There are two important issues with regard to the ozone distribution that should be emphasized. The first issue is the presence of a bias offset in the upper stratosphere between model calculations and data collected by SBUV, SAGE, and LIMS (models ranging from 30% to 50% lower in value). SAGE, SBUV, and LIMS were all operating at the same time in 1979, and comparisons have been made showing that in the region where models differ so much, the three

PHILOSOPHICAL TRANSACTIONS OF THE ROYAL SOCIETY A MATHEMATICAL, PHYSICAL & ENGINEERING SCIENCES

experiments agree to within about 10%. Because these three experiments are all different in measurement approach and wavelength region used, this gives strong confidence that the satellite observations are good to the *ca.* 10% level. Therefore, it leads further to the conclusion that there are fundamental problems with the model calculations that need to be resolved.

The second ozone issue is the Antarctic ozone 'hole' that was noted in the Introduction (Farman *et al.* 1985). A comparison of the preliminary total-ozone polar-stereographic projection obtained by SBUV for 30 September in 1985 and 1986 (A. J. Miller, personal communication) shows that on this day, the smallest value in 1986 is 30 Dobson units above the smallest 1985 value and the corresponding highs are significantly greater. This suggests a lessening of the depth of the hole. Examination of more data covering the winter–spring period confirms this suggestion. There is also evidence that smaller ozone values occur from year to year not only in the Antarctic region, but at lower latitudes as well. Figure 1 (from Schoeberl *et al.* 1986) shows zonal mean ozone for October measured by TOMS as a function of latitude for each year from 1979 to 1985. These results show that total ozone is decreasing over the 1979 to 1985 period from 30° S to the pole.

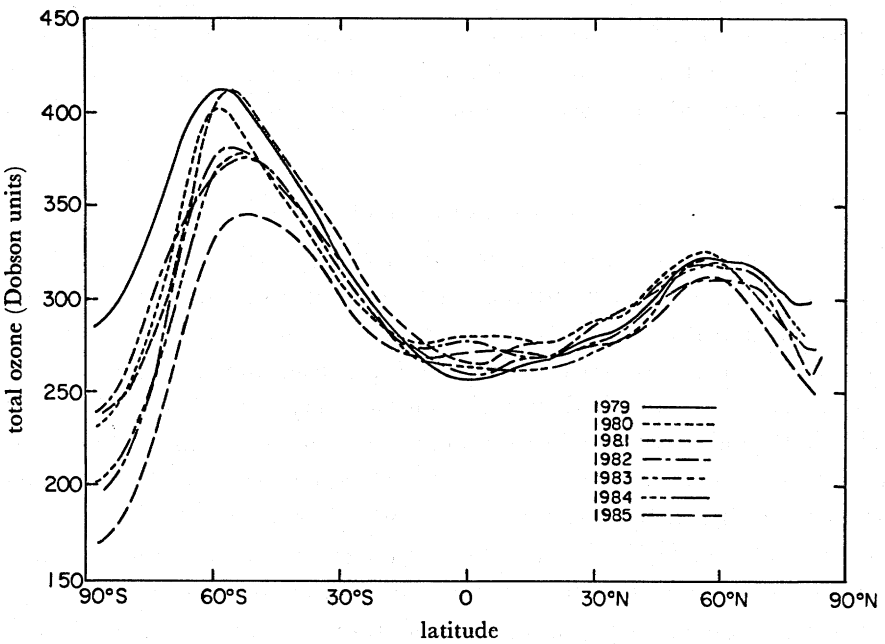

FIGURE 1. TOMS zonal mean total ozone averaged over the month of October against time for the time period 1979–1985 (from Schoeberl *et al.* 1986).

An important question regarding the occurrence of the ozone hole is the vertical extent of the depletion. Aikin & McPeters (1986) have investigated this by using SBUV data in the 75° S–80° S and 0°–60° W region by taking an ozone mean over five days in October for the years 1979–1984. The data cover the pressure interval from 30–0.7 mbar†, where SBUV data should have the best accuracy. Results show a decline in ozone from 1979 to 1984 on the order of 20% at all levels in the range 1–7 mbar. Some questions have been raised about the validity

† 1 mbar = 10^2 Pa.

PHILOSOPHICAL TRANSACTIONS OF THE ROYAL SOCIETY A MATHEMATICAL, PHYSICAL & ENGINEERING SCIENCES

of the SBUV algorithm for lower altitudes, but between the 7 mbar and 1 mbar levels, the data should be accurate (R. Hudson, personal communication).

There are numerous theories that have been advanced to explain the Antarctic ozone minimum involving, for example, dynamics, chlorine chemistry, heteorogeneous effects, and solar-cycle related NO_x chemistry. The body of evidence accumulated thus far, however, shows that the phenomenon is complex, and any theory must adequately address the results of the total data set including the findings of Schoeberl *et al.* (1986) and Aiken & McPeters (1986), i.e. ozone depletion outside the Antarctic region and depletion in the upper stratosphere. It is likely that coupled theories involving dynamics and chemistry interactions will have to be invoked to explain the total observations.

A final point on ozone that is unrelated to the two issues discussed above is worthy of note. A number of studies have been done to determine the relation, if any, between ozone change and short-term changes in the solar ultraviolet (UV). For a long time, there was no clear evidence of this coupling. Now, however, as a result of correlation studies between solar UV data from SBUV and ozone measurements collected by LIMS and SME, there is unmistakable proof of the interrelation (see, for example, Keating *et al.* 1986; Chandra 1986; Hood 1986). Keating *et al.* (1986) find ozone increases of 0.4% and 0.49% at 3 mbar (*ca.* 40 km) and 0.007 mbar (*ca.* 80 km), respectively, for a 1% increase in 205 nm solar radiation and a 0.14% ozone decrease at 0.04 mbar (*ca.* 70 km) for a 1% increase in Ly-α. The implications of these observations for photochemical studies and understanding of atmospheric processes needs to be thoroughly investigated.

Water vapour (H_2O)

Satellite observations of stratospheric water vapour have provided a significant step forward in our knowledge of the global distribution of this molecule and also our understanding of its vertical profile (see Russell *et al.* 1984; Remsberg *et al.* 1984; Jones *et al.* 1986). This knowledge has come primarily from the LIMS experiment and CH_4 measurements made by SAMS. Recently, four other experiments were launched that also measure H_2O: the Spacelab 1 grille spectrometer, SAGE II, SME, and ATMOS. Before the launch of *Nimbus* 7, only balloon and airborne *in situ* and remote observations had been made. Detailed reviews of these balloon-borne measurements were published by Harries (1976) and Ellsaesser (1983).

The monthly zonal mean H_2O concentration against latitude cross sections for November from LIMS is shown in figure 2. This figure shows the main features of the stratospheric H_2O distribution. It is characterized by a minimum in the tropics just above the tropical tropopause, a poleward mixing-ratio gradient at pressures up to the 4 mbar level, and then an equatorward gradient from that point to the stratopause. The distribution also has double minima in mixing ratio at about 4 mbar that, at times during the LIMS mission from October to May, merge into just one feature. Gray & Pyle (1986) have suggested that this behaviour is caused, in part, by the equatorial semiannual oscillation. Another characteristic of the distribution is an implied net circulation. The general picture suggested is a 'reservoir' of dry air in the tropics that is being carried upward and poleward as implied by the double minima with the strongest circulation being toward the winter pole (note that the 5 p.p.m.v. (parts per million by volume) contours close at *ca.* 6 mbar and 50° S in November, whereas this occurs at 60° N in May (not shown)). Also implied is a lower altitude poleward circulation from the Equator to the summer pole. The elongated contours at 80 mbar extending to 60° S support this idea, and it is consistent with data for other months in the LIMS mission.

PHILOSOPHICAL TRANSACTIONS OF THE ROYAL SOCIETY A MATHEMATICAL, PHYSICAL & ENGINEERING SCIENCES

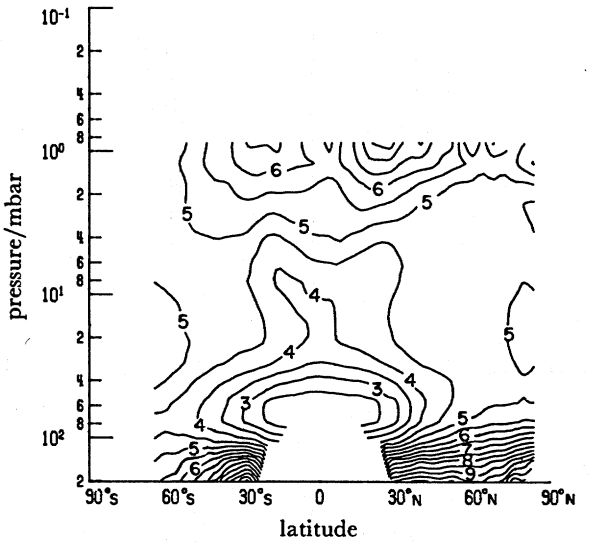

FIGURE 2. LIMS monthly zonal mean water vapour latitude cross section for November 1978 (contour interval is 0.5 p.p.m.v.).

Monthly zonal mean vertical H_2O profiles averaged over four latitude bands from 56° N to 84° N, 32° N to 56° N, 28° N to 28° S, and 32° S to 56° S are shown in figure 3 to provide another view of monthly changes (see Russell 1987). The high northern latitude profiles are characterized by very little change with altitude and the presence of an increase just above the tropopause in winter (see also figure 2).

This increase just above the tropopause also occurs in the Southern Hemisphere in May and is currently unexplained by models. Variations are similar for the northern mid-latitude range, but there is a slight trend of increasing mixing ratio with altitude. The tropical profiles are characterized by very small changes from month to month, a very pronounced minimum that occurs above the tropical tropopause, and a clear increase with altitude that is consistent with methane-oxidation theory. The minimum just above the tropopause was first observed in balloon soundings by Kley *et al.* (1979) who coined the phrase 'hygropause' to describe it. The mid-southern latitude profiles show an essentially constant mixing ratio with height above about 25 mbar, but there is significant variability below. A clear hygropause structure is present, probably because of the low altitude circulation carrying dry air from the tropics to the high latitudes. This structure gradually changes over the year up until May to a profile that is very similar to the November Northern Hemisphere profile. Various mechanisms have been proposed to describe formation of the hygropause (see Danielsen 1982), but at present, there is no consensus or agreed-upon process that adequately describes all available data.

Nitrogen dioxide (NO_2)

The most detailed description of the NO_2 global distribution was provided by LIMS, which collected data day and night at nominally 10h30 and 13h30 local time, providing *ca.* 7000 horizon scans each period of 24 h. The longest-running record of the NO_2 distribution has been provided by the SAGE, SAGE II, and SME experiments, which collected a more limited geographic data set, but one which spans a time period of several years. These experiments have produced some significant findings.

The main features of the global NO_2 distribution can be generally described by the LIMS day

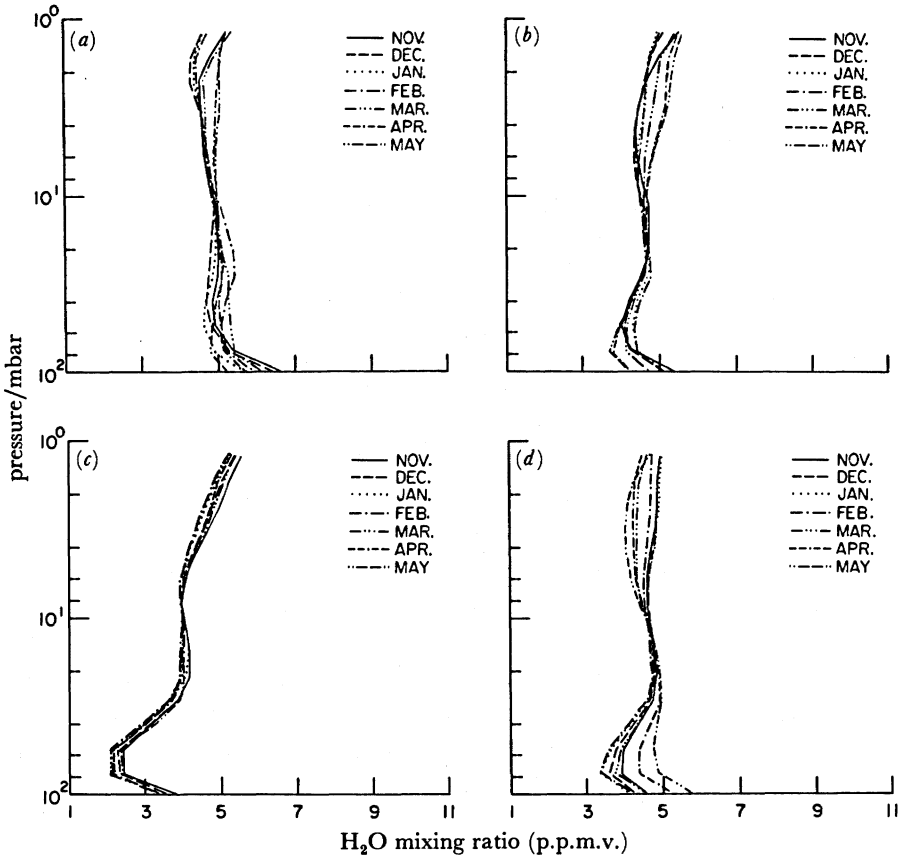

FIGURE 3. LIMS monthly zonal mean latitudinally averaged H_2O profiles for (*a*) 56° N–84° N, (*b*) 32° N–56° N, (*c*) 28° S–20° N, and (*d*) 32° S–56° S.

and night zonal mean distributions for January (figures 4 and 5, respectively). Note first figure 4, which shows that the daytime NO_2 distribution exhibits a layered structure with peak mixing ratios occurring approximately at the 7 mbar level. The peak value, *ca.* 7 p.p.b.v.,† occurs in the tropics and Southern Hemisphere. The shading is included to point out the region of the night terminator at *ca.* 68° N and the region below the 40 mbar altitude level where a climatology was used in the LIMS retrieval. This climatology was used to a progressively larger degree as altitude decreased. The climatological 'tie on' was necessary because of the steady loss of NO_2 signal and growth of molecular-oxygen continuum interference signal in that channel in the lower stratosphere. All of the archived NO_2 was retrieved in this way. The data in these shaded regions, therefore, should be interpreted cautiously in any science investigations. The night-time NO_2 distribution in figure 5 shows a similar character as the day, but the variations are enhanced. Note, too, that the maximum mixing ratio peaks further to the south and a hemispherically asymmetric behaviour exists the same as for the day. The zonal mean NO_2 distribution for other periods tends to be similar in form to the January cross sections. As time progresses from November to May, the Southern Hemisphere maximum region moves equatorward, and at the end of the LIMS mission in May the distribution is more nearly

† Parts per billion by volume; in this paper 1 billion represents 10^9.

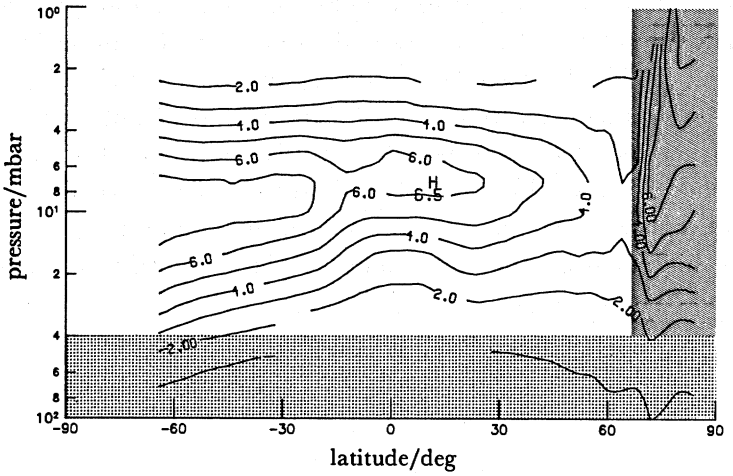

FIGURE 4. LIMS daytime monthly zonal mean NO_2 latitude cross section for January 1979 (contour interval is 1 p.p.b.v.).

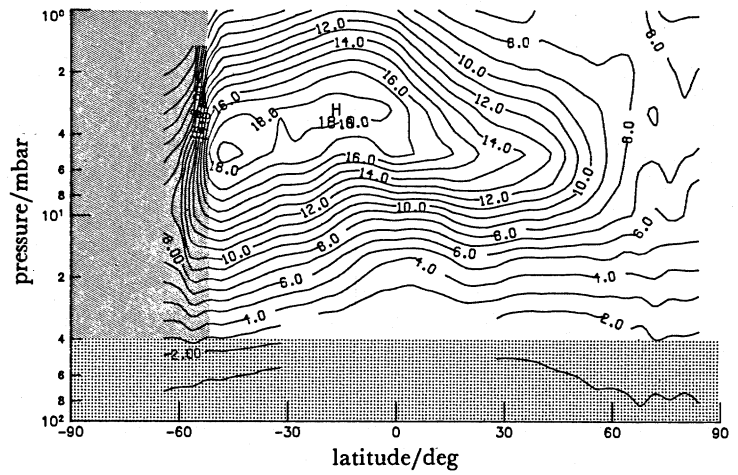

FIGURE 5. LIMS night-time monthly zonal mean NO_2 latitude cross section for January 1979 (contour interval is 1 p.p.b.v.).

symmetric about the Equator. There is still a southward displacement of the maximum region although not as much as in January.

A striking feature of the January night cross section is the large decrease in mixing ratio with increasing north latitude that, in the 5 mbar region, decreases from a maximum of *ca.* 19 p.p.b.v. in the tropics to 7 p.p.b.v. at 84° N. The polar stereographic projection for the same time period shows that the decrease occurs over a broad latitude–longitude region that coincides with the position of the north polar vortex. This phenomenon is a manifestation of the NO_2 behaviour first reported by Noxon (1979) and now commonly referred to as the 'Noxon cliff'. Its occurrence is believed to be caused by a steady conversion of NO_2 to N_2O_5 during the polar night as air makes circuits around the vortex going into and out of the night for varying time periods depending on latitude. Studies by Solomon & Garcia (1983) comparing model calculations to NO_2 amounts measured from the ground, and by Callis *et al.* (1983) comparing model results to LIMS observations, lend further support to this explanation.

The LIMS NO_2 retrievals were extended to a higher altitude by using radiance averaging techniques. As a result, in polar night, they extend to near the 70 km level and show large mixing-ratio values that are highly variable longitudinally (Russell *et al.* 1984) and that reach magnitudes of 175 p.p.b.v. at some locations. The data show that as time increases during polar night, mesospheric NO_2 increases and is subsequently transported downward into the stratosphere. The implied downward velocity of *ca.* 1 cm s^{-1} at the stratopause is in accord with predictions. Figure 6*a*, *b* present five-day zonal means during late January and early February 1979 showing that the high mesospheric polar night NO_2 levels (northward of 60° N) dissipate fairly quickly after polar night ends.

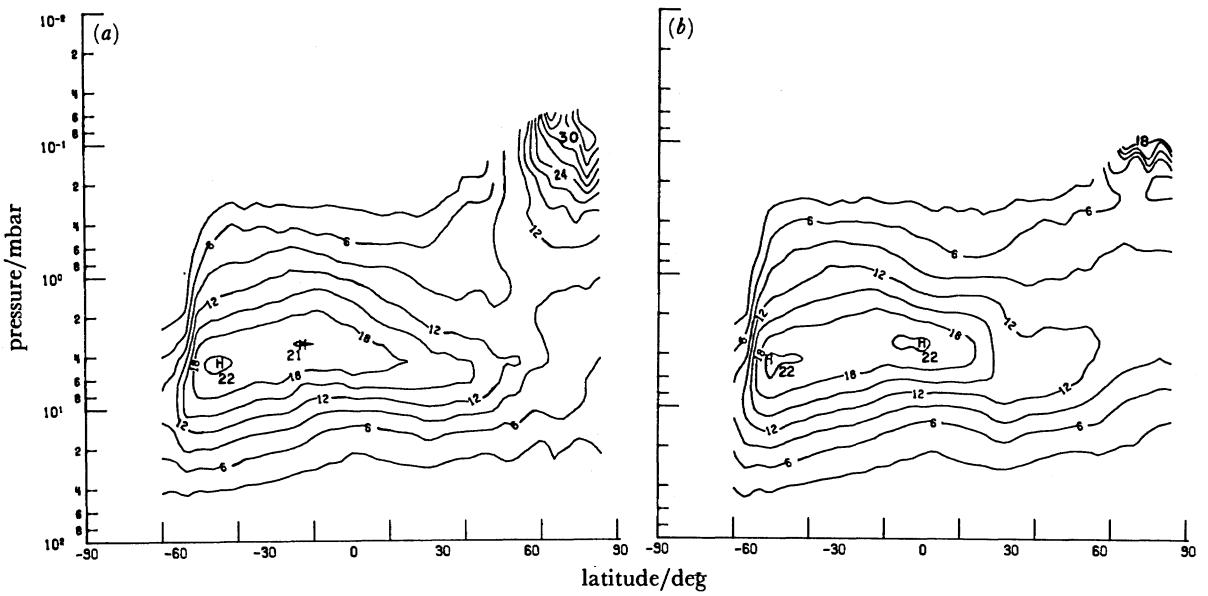

FIGURE 6. LIMS night-time radiance averaged zonal mean NO_2 latitude cross section for (*a*) 19–23 January 1979 and (*b*) 7–12 February 1979 (contour interval is 3 p.p.b.v.).

Nitric Acid (HNO_3)

The only available satellite measurements of HNO_3 were obtained by the LIMS experiment, which made observations over the entire 7.5 month time period of operation. The data cover from the tropopause to near the stratopause level and include the northern polar night. The distribution over this time can be characterized by the January and May zonal mean pressure against latitude cross sections shown in figure 7. The zonal mean distributions show a region of low values of nitric acid at all altitudes near the Equator and a rather sharp poleward gradient with increasing mixing ratios toward both poles at levels up to about 20 mbar. There is a hemispheric asymmetry (of *ca.* 3 p.p.b.v. for 60° N and 60° S), with the highest levels of HNO_3 occurring in the high-latitude winter hemisphere. This asymmetry is not currently reproduced by either two-dimensional or three-dimensional model calculations and represents a major unresolved question regarding odd nitrogen processes in the polar night and high-latitude winter region. The altitude slope in the winter hemisphere (or fall for May Southern Hemisphere data) slopes upward and poleward above 20 mbar. The summer hemisphere slope is very shallow in that region. Below the 20 mbar level, the slope is poleward and downward at all times for both hemispheres.

PHILOSOPHICAL TRANSACTIONS OF THE ROYAL SOCIETY A MATHEMATICAL, PHYSICAL & ENGINEERING SCIENCES

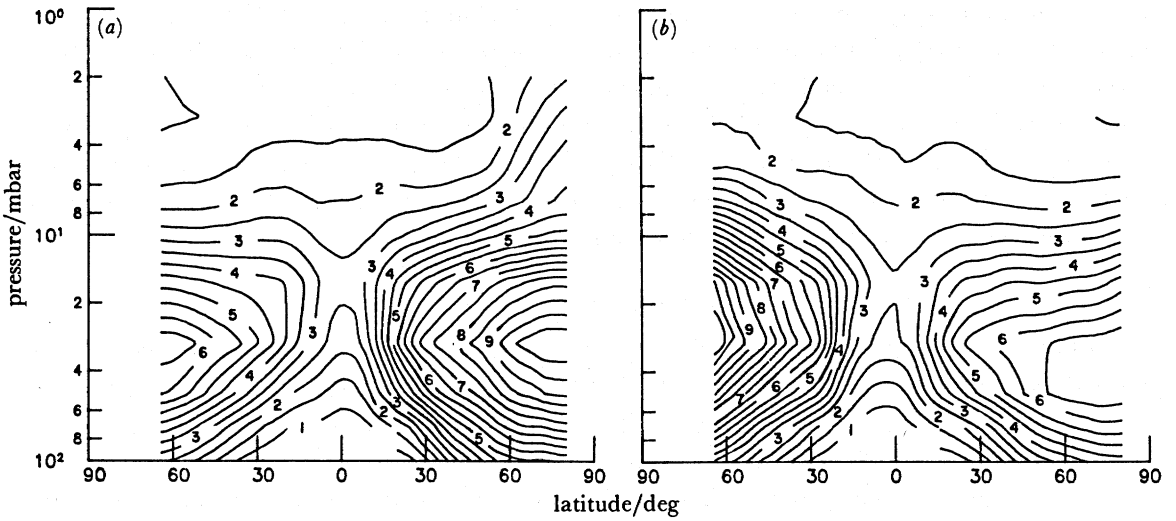

FIGURE 7. LIMS monthly zonal mean HNO_3 latitude cross section for (*a*) January and (*b*) May 1979 (contour interval is 0.5 p.p.b.v.).

The data for the 30 mbar level, where the maximum HNO_3 mixing ratio occurs, show that HNO_3 is highly variable longitudinally in winter, but in spring, the variations are greatly reduced. The largest changes occur at mid- and high latitudes in January where wavenumber 3 and 4 patterns can be seen clearly. The Northern Hemisphere winter at latitudes above *ca.* 60° N is characterized by fairly rapid variations that begin to decrease just after the major warming is over near the end of February. This time also marks the beginning of the reversal in asymmetry.

An interesting feature of the zonal mean latitude cross section is the presence of enhanced HNO_3 values northward of *ca.* 55° N and above the 10 mbar level. This can be seen in figure 7*a* as distinct changes in the contour slopes at about the 7 mbar level. Detailed examination of the data shows that this feature occurs only in polar night. There appears to be a slight enhancement beginning in May in the same region of the Southern Hemisphere as is the case for November in the North; but the LIMS data do not extend far enough southward or in time to confirm this. Time-series analyses at several pressure levels show that this feature is clearly a high-altitude polar-night phenomenon, which slowly increases with time during the night, but decreases rather sharply once sunlight returns (Austin *et al.* 1986). It is also strongly altitude dependent, with essentially no effect seen at the 8.3 mbar level. It sometimes forms as low as the 10 mbar level. The decrease after sunlight returns is present also at 11.4 mbar as well. This feature and its behaviour suggest the presence of an unknown source for nitric-acid formation. The pressure level where it begins to form coincides with the region where NO_2 decreases to very low values, presumably because of conversion to N_2O_5. This has led Austin *et al.* (1986) to speculate either on a gas-phase reaction of N_2O_5 with H_2O, or aerosols as potentially important HNO_3 sources. These authors conclude that the gas-phase reaction rate required to explain observations is too large based on available data.

One final point to be made on HNO_3 is its response to solar UV variations. This has been studied in some depth by Keating *et al.* (1986) who used LIMS HNO_3 data and SBUV measurements of short-term changes in the 205 nm UV flux. They compared five-day running mean fractional changes in the solar uv flux with fractional changes in the 10 mbar level five-day

running mean HNO_3 mixing ratio. The fractional change for both HNO_3 and the solar flux were computed relative to the nineteen-day mean and averaged over the 40° S–40° N latitude range. Their results show an anticorrelation of solar UV change against HNO_3 change, and the correlation coefficient (-0.78) is a maximum when the lag between HNO_3 response and solar UV change is 0 ± 1 day. The HNO_3 appears to be greater than a factor of two more sensitive to UV changes than is ozone. Comparison of these changes to model calculation variations performed by the authors shows fair agreement.

Total odd nitrogen (NO_y)

In all of the ozone depletion scenarios resulting from chlorine, the role of NO_y compounds (defined here as $NO + NO_2 + HNO_3 + 2 \times N_2O_5 + HNO_4 + ClONO_2$) is very important because the NO_y species act to buffer the effect of ClO_x on ozone destruction. Therefore, a good understanding of the global NO_y distribution is crucial.

The LIMS experiment has provided information on the lower limit of NO_y through night-time measurements of NO_2 summed with nitric acid. Figure 8 shows monthly zonal mean cross

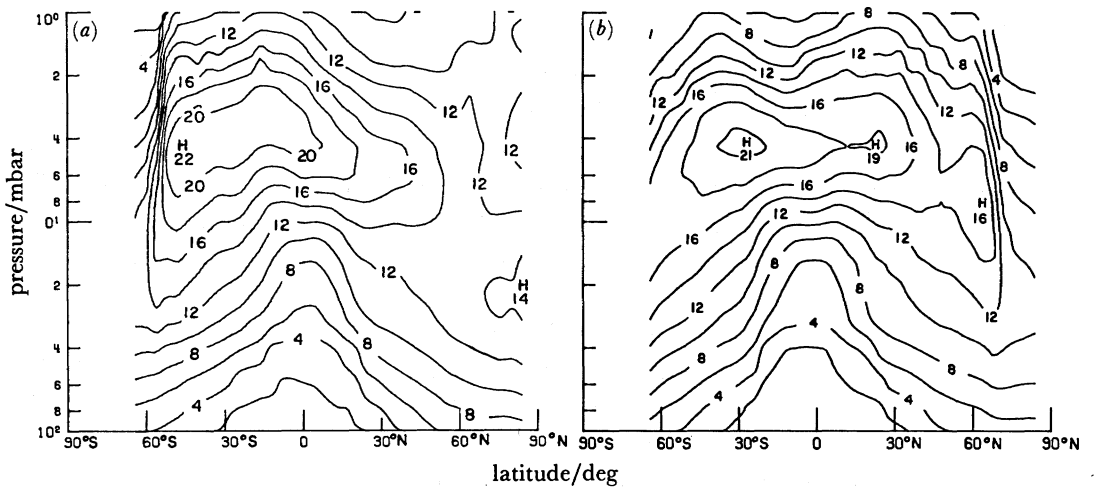

FIGURE 8. LIMS night-time monthly zonal mean $NO_2 + HNO_3$ latitude cross section for (*a*) January 1979 and (*b*) May 1979 (contour interval is 2 p.p.b.v.).

sections of $NO_2 + HNO_3$ for January and May 1979. There are several points to note from these figures. First, it should be pointed out that the sum is primarily governed by night-time NO_2 levels (see figure 5). There is also significant variability in the sum both with latitude for a given month and with time. Notice that in May, the maximum $NO_2 + HNO_3$ region is more symmetric about the Equator than in January, and maximum mixing ratio levels extend to higher northern latitudes. The highest level in January is 22 p.p.b.v., which occurs at 55° S, and in May it is 21 p.p.b.v. occurring at 30° S. The minimum value at the altitude level where peak mixing ratio occurs is about 12 p.p.b.v. and occurs at 60° north and south latitude. Lower values than this exist in the data set, but these occur because the measurement path crosses the terminator into daylight where NO_2 levels are much lower. Longitudinal variability is also large. The data for 1 May 1979 at 48° S (not shown), for example, show that the sum of $NO_2 + HNO_3$ varies from 17 p.p.b.v. to 27 p.p.b.v. around a longitude circle. Similar variations

are observed in the Northern Hemisphere high-latitude winter region. This implied spatial variability suggests that two-dimensional and three-dimensional models (as opposed to one-dimensional) are required to adequately simulate observed distributions.

Methane (CH_4) *and nitrous oxide* (N_2O)

These two molecules are discussed extensively in another paper in this symposium by Taylor & Dudhia. Therefore, the salient features of the distributions, their spatial and temporal variations, and the implications of the data will not be described here. There are some points, however, concerning correlations between LIMS H_2O and SAMS CH_4 and N_2O distributions that are worthy of note.

It was pointed out earlier that the H_2O zonal mean latitude cross section shows a double minimum structure in the mid- and upper stratosphere. The N_2O and CH_4 results show similar features, but they are double maxima instead, and they are closely correlated with the H_2O field. These data sets are compared for the month of May in figure 9. There is very good agreement in the location of the double minima and double maxima for the two data sets, providing strong evidence that the features are real. The CH_4 and H_2O data especially show the correlations. Where CH_4 and N_2O mixing ratios are large, H_2O values are small, and vice versa. This picture supports the idea of a net circulation that carries CH_4-rich and N_2O-rich air from the tropospheric source region upward and then branches north and south, while at the same time carries H_2O-poor air to higher levels from the tropical 'dry reservoir' (hygropause region) in the lower stratosphere. This picture needs to be thoroughly investigated because it should shed light on the general stratospheric circulation. Studies of the kind performed by Solomon *et al.* (1986*b*) for CH_4 and N_2O, but carried out for H_2O, would be helpful. The major problem in doing a study like this, however, is in knowing the H_2O flux across the tropopause boundary, which is very poorly understood at present.

The correspondence of CH_4 and H_2O shown by SAMS and LIMS data led Jones *et al.* (1986) to examine the sum $2\times CH_4+H_2O$, which should closely approximate the total hydrogen content of the stratosphere. If there are no losses of water from the stratosphere from heterogeneous processes, then total hydrogen should be conserved in the CH_4 oxidation process forming water vapour, and by examining the sum as a function of altitude and latitude, the methane oxidation theory can be tested. The neglect of molecular hydrogen in the study should have only a small effect on conclusions because it appears, based on available data, to be constant with altitude and has a mixing ratio of only about 0.5 p.p.m.v. (NASA/WMO 1986). The authors showed that for the 30–40 km region, the sum of $2\times CH_4+H_2O$ is, on the average, about 6 ± 0.5 p.p.m.v. for all months, altitudes, and locations when LIMS and SAMS were operating simultaneously. The fact that the sum is so constant in time and spatial location leads to the conclusion that CH_4 oxidation is the dominant source for *in situ* formation of stratospheric water vapour.

Other molecules

The SAMS experiment, the Spacelab 1 grille spectrometer, and ATMOS all measured carbon monoxide in the stratosphere and mesosphere. Carbon monoxide is of interest in the middle atmosphere primarily because of its role as a tracer for study of middle-atmosphere transport. Ground-based observations with microwave techniques (Clancy *et al.* 1984) and two-dimensional model calculations (Solomon *et al.* 1985*b*) suggest that CO mixing ratios are higher in

PHILOSOPHICAL TRANSACTIONS OF THE ROYAL SOCIETY A MATHEMATICAL, PHYSICAL & ENGINEERING SCIENCES

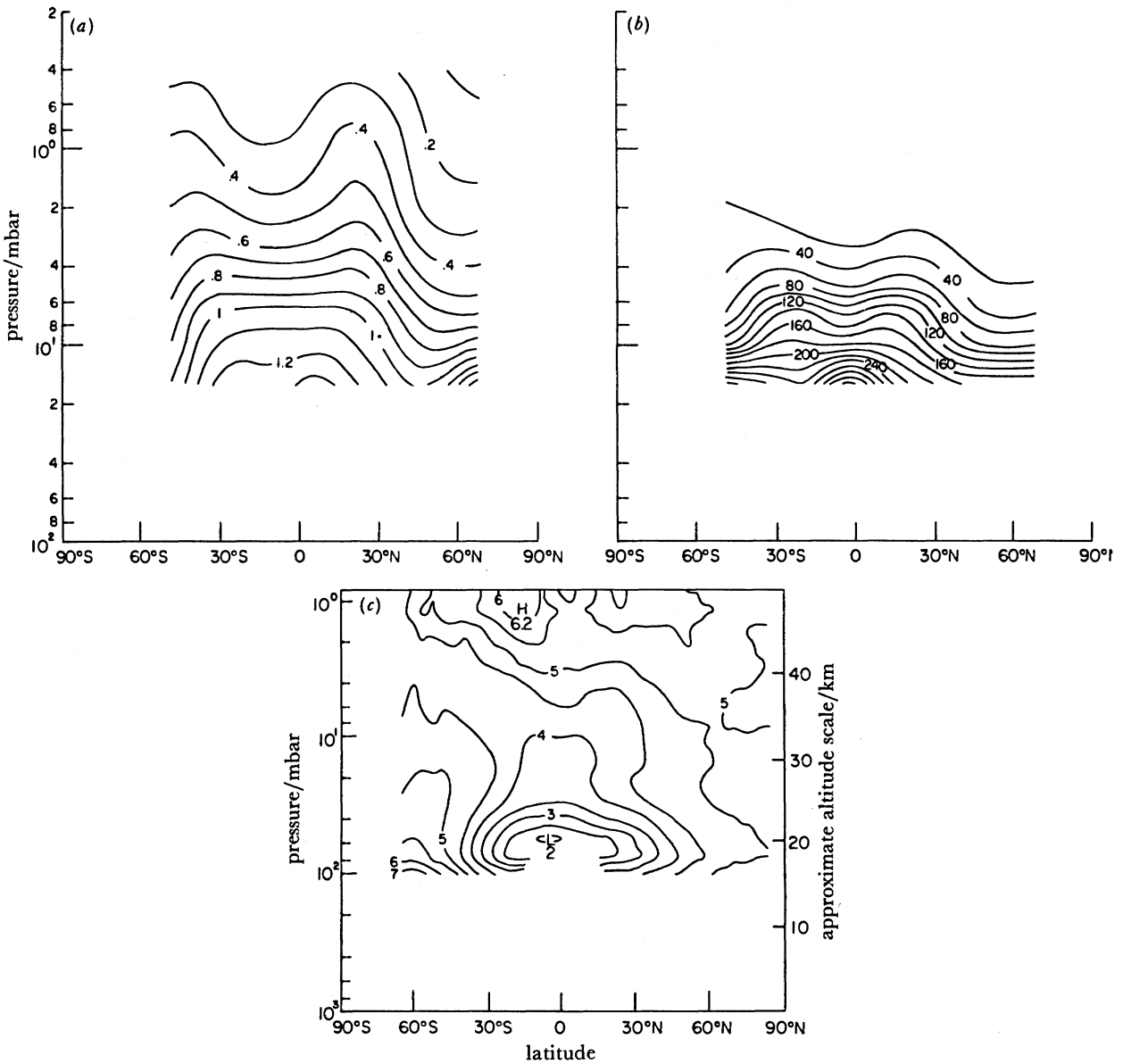

FIGURE 9. Comparison of SAMS CH_4 and N_2O zonal mean latitude cross sections with LIMS H_2O data for May 1979. (*a*) SAMS CH_4 (0.1 p.p.b.v. intervals); (*b*) SAMS N_2O (20 p.p.b.v. intervals); (*c*) LIMS H_2O (0.5 p.p.m.v. intervals).

the winter mesosphere than in summer primarily because of downward transport by the mean meridional circulation. Figure 10 shows a comparison of the grille spectrometer sunrise and sunset data with SAMS results averaged over a time period of six months and over the 35° N–70° N latitude range. The averaging was necessary because of low signal:noise ratio. SAMS data are considerably higher than the grille spectrometer results except near the sunset peak. ATMOS data, which are not yet published, confirm the general seasonal dependence suggested by figure 10 and other data.

The ATMOS science team has recently reported on observations from Spacelab 3 of four key stratospheric molecules that previously had not been measured. These include N_2O_5 (Toon

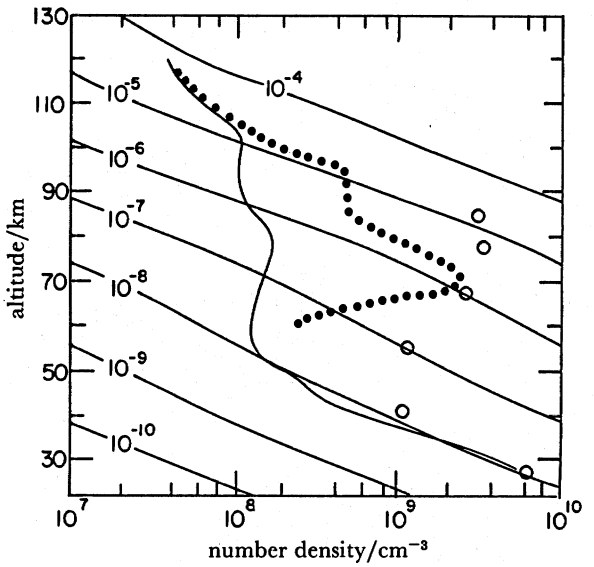

FIGURE 10. Carbon monoxide measurements made by the Spacelab 1 grille spectrometer at sunrise on 3 December 1983, 68° S (solid) and sunset on 29 November 1983, 44° N (dots) (from Lippens *et al.* 1984) compared with SAMS measurements (open circles) averaged over 35° N–70° N and January–June 1979 (from Jones & Pyle 1984).

et al. 1986), $ClONO_2$ (Zander *et al.* 1986), HNO_4 (Rinsland *et al.* 1986*a*), and COF_2 (Rinsland *et al.* 1986*b*). A fifth gas, methyl chloride (CH_3Cl) was also measured for the first time from a satellite, thus demonstrating the potential for global scale observations of this important chlorine source molecule (Park *et al.* 1986). The clear identification of absorption by N_2O_5 in the ATMOS data is a significant measurement advance. Its presence in the atmosphere has been speculated on using NO_2 observations (Solomon & Garcia 1983; Callis *et al.* 1983, 1986; Russell *et al.* 1984) and diurnal measurements in the 1230–1250 cm^{-1} region made from a balloon platform (Roscoe 1982). The implied peak N_2O_5 mixing ratio retrieved from the ATMOS data is *ca.* 1.6 p.p.b.v. at *ca.* 35 km. The estimated error in the measurement of $\pm 50\,\%$ is dominated by uncertainty in integrated band intensity. Peak mixing-ratio values and altitudes for $ClONO_2$, HNO_4, COF_2, and CH_3Cl are 1.4 ± 0.7 p.p.b.v. at 28 km, 0.35 ± 0.15 p.p.b.v. at 26 km, 0.1 ± 0.05 p.p.b.v. at 32 km, and 0.65 ± 0.19 p.p.b.v. at 12 km, respectively. In each case, the dominant error source is uncertainty in the absorption data.

Aerosols

An extensive set of aerosol data has been collected by the SAM II, SAGE, and SAGE II series of satellite experiments, which span many years and a wide latitude range. A spring 1979 seasonal zonal mean for SAGE aerosol data is shown in figure 11. (The SAGE lifetime was February 1979–November 1981). It is constructed from all the $\lambda = 1\ \mu m$ aerosol extinction profiles obtained during the months of March, April and May 1979. The upper panel, figure 11*a*, plots the zonal mean of these profiles in units of 10^{-5} km^{-1}. The diamonds indicate the zonal mean-tropopause height. This period in 1979 was one of very low aerosol loading with very little volcanic residue, and is considered representative of a background condition. Extinction coefficient values of about 10^{-4} km^{-1} in the main stratospheric layer, slightly above the tropopause to about 25 km, are typical. Figure 11*b*, which is the ratio of aerosol extinction to

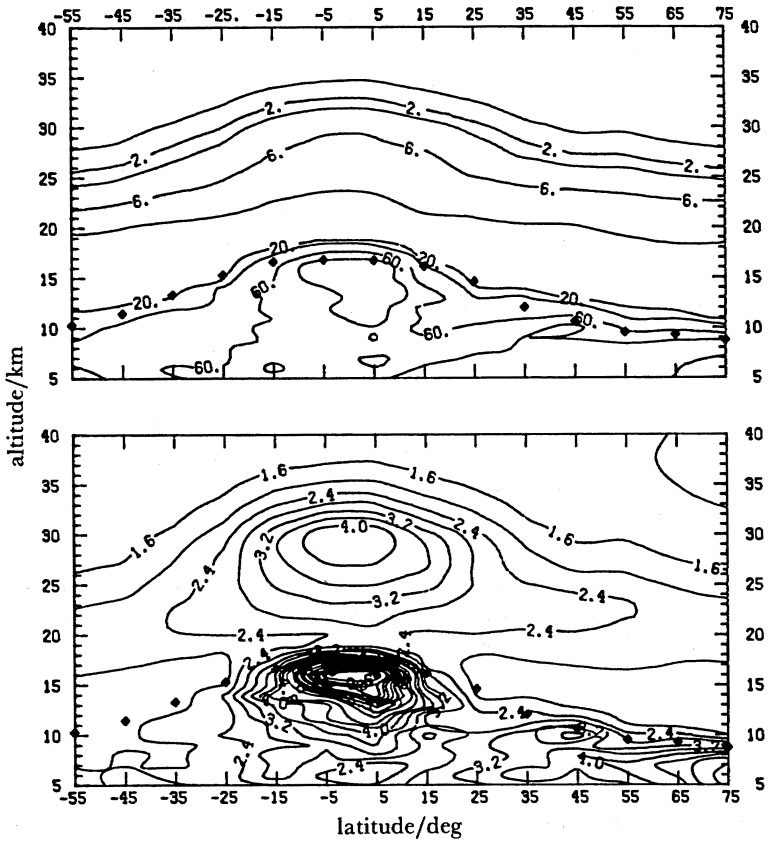

FIGURE 11. Zonally averaged SAGE aerosol extinction and extinction ratio at $\lambda = 1.0$ μm for March–April–May 1979.

molecular extinction, is similar to a mixing ratio. The peak values of this extinction ratio reside in the tropics indicating this to be the source region for stratospheric aerosols. SAGE data for the other seasons of 1979 are given in McCormick (1985). The background aerosol level of the stratosphere changes dramatically for volcanic conditions powerful enough to put material into the region. A good example of this is given in figure 12, which shows SAGE extinction profiles at $\lambda = 1$ μm integrated in altitude from 2 km above the tropopause upward to 35 km to produce stratospheric aerosol optical depths at the beginning, during, and after the Mount St Helens eruption. SAGE was making measurements at about 70° N at the time of the eruption on 18 May 1980.

The top panel of figure 12 presents SAGE observations as its measurement location moved southward from about 70° N on 12 May to 45° S on 20 June. Each day, 15 sunset profiles of extinction are made. The optical depth shading is shown on the bottom of the figure. Initially, a large amount of fine dust, sulphuric-acid aerosol, and SO_2 gas are emitted into the stratosphere. The material above about 20 km experienced an easterly wind blowing this material toward the Pacific, whereas the material below 20 km moved east and southeast over Canada and the U.S.A. The bottom panel, for the period 21 July–26 August, shows the effects of gas-to-particle conversion and the 'smoothing out' of the aerosol through various mixing and diffusion processes. Note that most of the material resided in the Northern Hemisphere at that time.

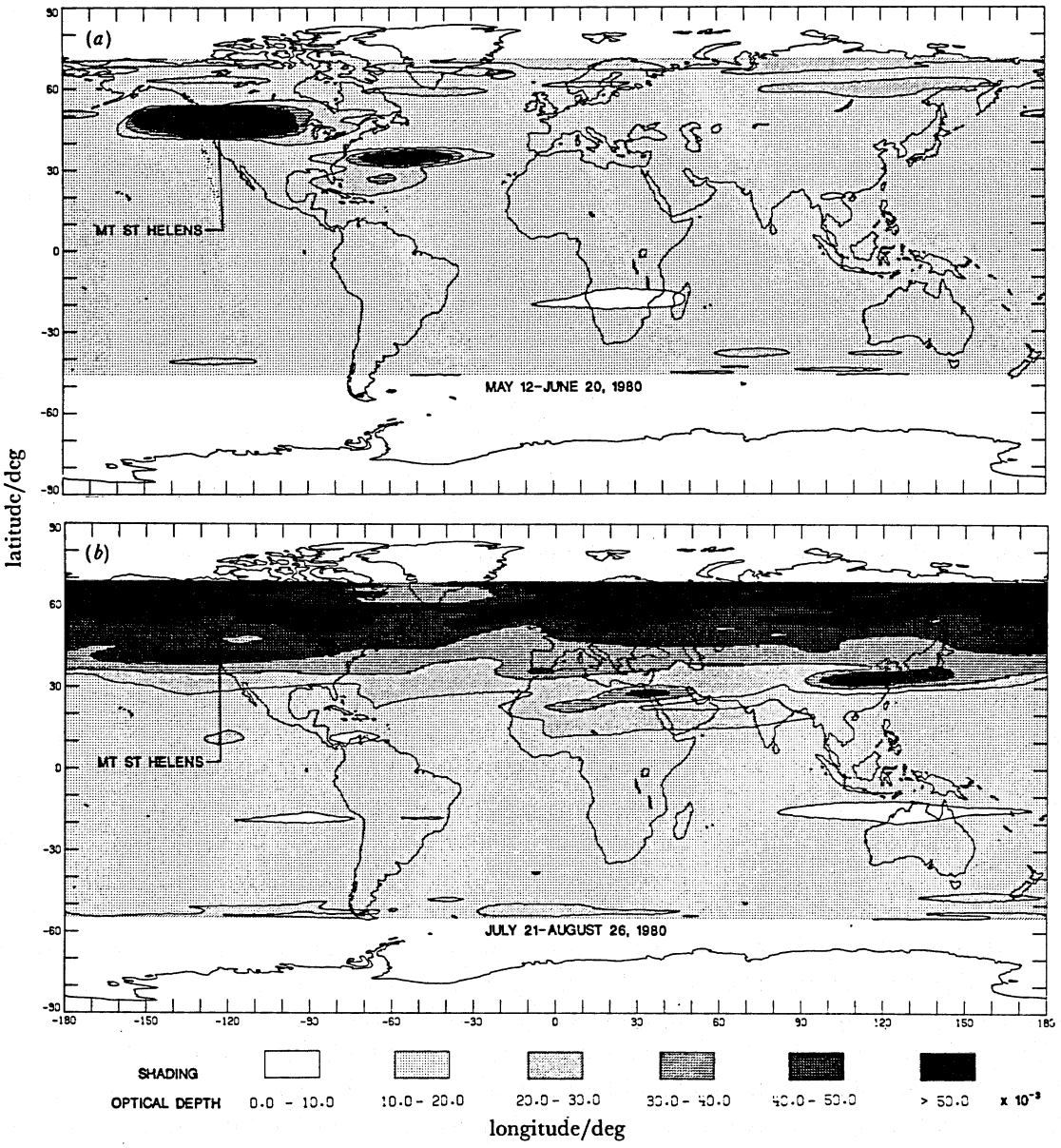

FIGURE 12. Aerosol optical depth at $\lambda = 1.0$ μm following the eruption of Mt St Helens in May 1980 calculated from SAGE extinction profiles integrated from the tropopause plus 2 km through the stratospheric aerosol layer.

SAGE made its measurements between about 72° N and 72° S because of its highly precessing 56° inclined orbit. SAM II, however, is in a high-noon sunsynchronous orbit aboard *Nimbus* 7 and, therefore, makes all its measurements in the polar regions. Sunset measurements occur between 64° N and 80° N, and sunrise measurements occur between 64° S and 80° S. The minimum and maximum latitudes are reached at solstice and equinox, respectively. Figure 13 presents the weekly averaged SAM II, $\lambda = 1$ μm, optical depth record from launch in October 1978 until the end of 1985 calculated from 2 km above the troposphere through the stratosphere.

The Arctic data are shown with a broken line and the Antarctic data with a solid line.

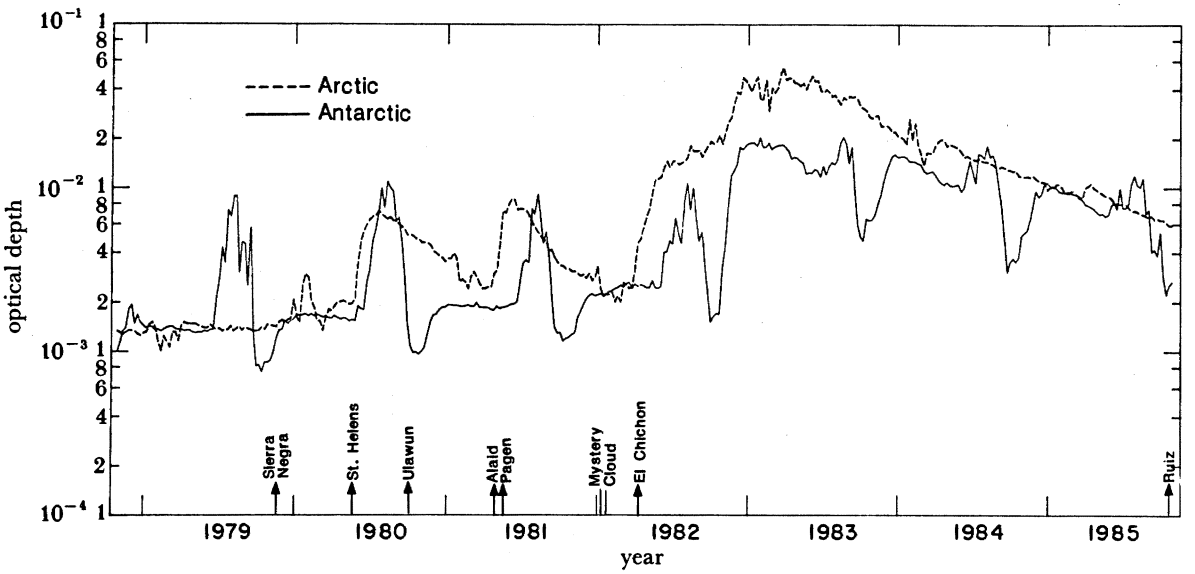

FIGURE 13. Aerosol optical depth at $\lambda = 1.0\ \mu m$ calculated from SAM II extinction profiles integrated from the tropopause plus 2 km through the stratospheric aerosol layer. SAM II Arctic data are averaged over 64° N–80° N, and the Antarctic data are averaged over 64° S–80° S. Noted are dates of volcanic eruptions known to have impacted stratospheric aerosols.

Annotated on the abscissa are the dates of major volcanic eruptions. SAM II remains operational at the time of writing this paper (November 1986). The effects of Mount St Helens were observed in the Arctic very soon after its eruption. After this, the effects from a number of eruptions were observed, with the largest perturbation occurring because of the eruption of El Chichon on 4 April 1982. The peak values were observed in January–March 1983. The peak optical-depth values of about 0.06 in figure 13 are conservative with individual measurements reaching well over 0.1. The Arctic values are about 40 times greater than the early 1979 values. El Chichon produced probably the largest impact on the Northern Hemispheric stratospheric aerosol experienced in this century (McCormick *et al.* 1984), impacting remote sensors (Bandeen & Fraser 1982), stratospheric temperatures (Labitzke *et al.* 1983), trace species (Mankin & Coffey 1984), and possibly tropospheric temperatures and El Nino events (Handler 1984).

As can be seen in figure 13, Alaid and Pagan both erupted within a month of each other in 1981. Most of the injected material from Pagan, however, remained at low latitudes and was not transported to high northern latitudes during the summer months (Kent & McCormick 1984). The increased optical depth in figure 13, therefore, should be attributed to Alaid. Similarly, the eruption of Ulawun in October 1980 had little effect at high latitudes. Thus, it becomes evident that the impact of an eruption at a particular latitude band is dependent on the location and season of the particular eruption.

Also evident in the northern optical-depth record are relatively small enhancements that occur every winter. These enhancements in optical depth are from attenuation caused by clouds in the lower stratosphere; these have been generically named polar stratospheric clouds (PSCs) by McCormick *et al.* (1982). They are found in the cold polar vortex and are thought to be made up of ice particles. The Antarctic optical depths clearly show the PSC enhancements occurring each Austral winter. Here, with a much more stable and larger vortex of colder winter stratospheric air, PSCs are more numerous. In general, PSCs exist when the temperature falls below about 200 K with a greater than 50% probability of occurrence for temperatures

below about 194 K. Although SAM II measurements are fixed in latitude on a particular day, airborne lidar missions have shown that PSCs do exist at other locations within the vortex where these cold temperatures exist (McCormick *et al.* 1982).

During early October, the SAM II geometry is such that most of its Antarctic measurements occur well within the polar vortex with very little aerosol observed. At this time, a yearly

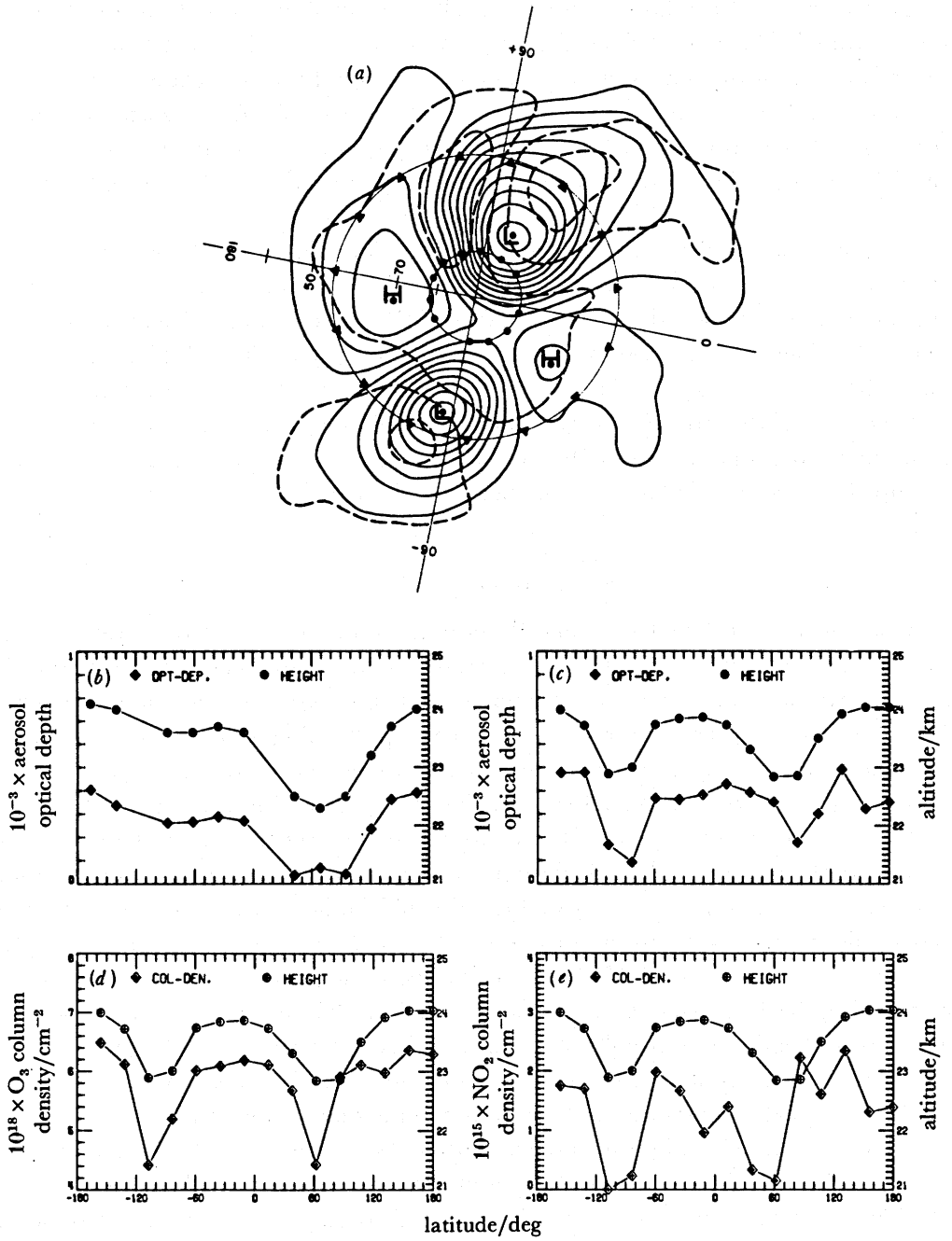

FIGURE 14. (*a*) The 30 mbar geopotential height and temperature field for 25 February 1979. SAM II and SAGE measurement locations are denoted by ● and ▲, respectively; (*b*) SAM II aerosol optical depth above 50 mbar; (*c*) SAGE aerosol optical depth above 50 mbar; (*d*) SAGE ozone column density above 50 mbar; (*e*) SAGE NO_2 column density above 50 mbar. Also plotted in (*b*)–(*e*) is the corresponding height of the 30 mbar pressure level.

minimum in vertical optical depth is observed (see figure 13). This pattern is repeated each year, even during periods of high volcanic loading. This occurs because after the polar vortex is formed in the stratosphere, mixing is severely inhibited causing a quasi-isolation of the aerosol. Air-mass subsidence occurs during this period, as does sedimentation of the particles, both of which cause a lowering of the aerosol-concentration profile; and over time, this leads to an overall decrease in overhead loading. Once most of the PSCs evaporate in late September, the remaining aerosols are at a relative minimum. This became very clear from the analysis by Kent & McCormick (1984) that showed that when aerosols from the low latitude eruption of Sierra Negra arrived in the northern polar region, they could not penetrate the vortex above 14 km. Rates of subsidence were calculated by tracking aerosols in the vortex against time (Kent *et al.* 1985). In addition, an airborne lidar mission across the Arctic vortex showed clear evidence of this isolation in aerosols between the inside and outisde of the vortex (McCormick *et al.* 1983).

This isolation effect has also been seen in ozone and NO_2. Figure 14 shows SAM II and SAGE measurements of aerosol, ozone, and NO_2 on 25 February 1979, with the corresponding 30 mbar geopotential height and temperature field. Minimum columns of aerosols, ozone, and NO_2 are clearly shown to exist within the two low-pressure systems, with high values outside these lows. The same kind of isolation also exists for a singular low-pressure system.

After breakdown of the Antarctic vortex, material from lower latitudes, previously isolated from inside the vortex, moves into the higher latitude regions. This is also shown in figure 14 by the abrupt increase seen in early November of each year.

Concluding remarks

In this paper we have provided a summary of current knowledge of stratospheric composition measured remotely from satellites. Indeed, much has been learned and many questions have been raised. The most notable phenomenon, observed first from the ground and then elucidated by satellite observations, is the Antarctic ozone hole. A perplexing aspect of the ozone data set is the significant discrepancy between satellite observations and models in the 40 km region. The reasons for the differences (model ozone is low compared with data) are still not understood, and in view of the agreement of the various satellite data sets, the differences point to fundamental problems with model calculations or reaction rate data. Remote observations of atomic oxygen or the atomic oxygen:ozone ratio would be helpful in studying this question.

The polar night of both hemispheres has proven to be a region of special interest. For example, the apparent source of HNO_3 in polar night, alluded to earlier, has no proven explanation. Also, the 7 mbar HNO_3 secondary maximum that occurs only during polar night is not understood. Another polar-night phenomenon that has been observed in only one winter in the north is the mesospheric NO_2 source. Although this feature seems to be fairly well understood theoretically, observations over more than one winter and at both poles are essential. An associated polar-night phenomenon that also appears to be fairly well understood based on comparisons of data with trajectory and three-dimensional model calculations is the NO_2 cliff. The most important missing links to test theoretical explanations of these phenomenon are a global data set describing the N_2O_5 distribution, especiallly at high winter latitudes, and improved data on heterogeneous reaction rates. It would also be helpful to have satellite observations at high southern winter latitudes to provide data for comparison with Arctic results.

PHILOSOPHICAL TRANSACTIONS OF THE ROYAL SOCIETY A MATHEMATICAL, PHYSICAL & ENGINEERING SCIENCES

The SAM II, SAGE, and SAGE II satellite programs are providing an evolving global aerosol climatology picture. In general, five major zones are evident in the data; three relative maxima at 75° S–40° S, 20° S–20° N and 40° N–75° N, and two relative minima at 40° S–20° S and 20° N–40° N. The background value (non-volcanic conditions) of total global aerosol loading has been determined to be 0.5×10^{12} g (0.5 Mtonne). The long-term trend in stratospheric aerosols appears to be governed by volcanic perturbations, with the latitude and altitude of the eruption and season being important to when and where the material is mixed. The polar regions show a large variability in aerosols dependent on the stratospheric polar vortex location and temperature. Aerosol-tracer studies have shown that the vortex restricts the movement of aerosols, preventing them from being transported into the vortex from outside at altitudes above about 14 km. Similar results for O_3 and NO_2 have been observed by SAGE and SAGE II. Polar stratospheric clouds have been identified and are observed to be a localized phenomena occurring in the cold winter polar vortex of both hemispheres.

In summary, there has been a quantum step of information provided by satellites on the global distribution and variability of trace-gas distributions and aerosols in the middle atmosphere. Much has been learned and, as usually is the case, many new questions have been raised; but definite scientific progress has occurred. Although a comprehensive data base exists, there are deficiencies in the existing data set, particularly regarding species in the Cl_x and HO_x family. It is anticipated that the upper atmosphere research satellite, which is to be launched early in the next decade, will provide new data on Cl_x simultaneously with measurements of the NO_x compounds measured previously. There will remain, however, the need to measure N_2O_5 globally as well as key members of the HO_x family (i.e. OH, HO_2, and H_2O_2) and atomic oxygen.

We acknowledge the helpful comments of Ellis E. Remsberg and Susan Solomon on the manuscript, the sharing of unpublished ozone data by A. J. Miller, and the diligent preparation of the typescript by Sheila D. Johnson.

References

Aikin, A. C. & McPeters, R. D. 1986 *Geophys. Res. Lett.* **13**(12), 1300–1303.
Austin, J., Garcia, R., Russell, J. M. III & Solomon, S. 1986 *J. geophys. Res.* **91**(D5), 5477–5485.
Bandeen, W. R. & Fraser, R. S. 1982 *Radiative effects of the El Chichon volcanic eruption: preliminary results concerning remote sensing*. NASA technical memorandum no. 84959.
Barth, C. A., Rusch, D. W., Thomas, R. J., Mount, G. H., Rottmon, G. J., Thomas, G. E., Saunders, R. W. & Lawrence, G. M. 1983 *Geophys. Res. Lett.* **10**, 237–240.
Callis, L. B. & Natarajan, M. 1986 *J. geophys. Res.* **91**(D10), 10 771–10 796.
Callis, L. B., Russell, J. M. III, Haggard, K. V. & Natarajan, M. 1983 *Geophys. Res. Lett.*, **10**(10), 945–948.
Callis, L. B., Natarajan, M., Boughner, R. E., Russell, J. M. III & Lambeth, J. D. 1986 *J. geophys. Res.* **91**(C1), 1167–1197.
Chandra, S. 1986 *J. geophys. Res.* **90**(D1), 2331.
Clancy, R. T., Muhleman, D. O. & Allen, M. 1984 *J. geophys. Res.* **89**(D6), 9673–9676.
Danielsen, E. G. 1982 *Geophys. Res. Lett.* **9**, 605–608.
Ellsaesser, H. W. 1983 *J. geophys. Res.* **88**(C6), 3897–3906.
Farman, J. C., Gardiner, B. G. & Shanklin, J. D. 1985 *Nature Lond.*, **315**, 207–210.
Farmer, C. B. & Raper, O. F. 1986 High resolution infrared spectroscopy from space: a preliminary report on the results of the atmospheric trace molecule spectroscopy (ATMOS) experiment on Spacelab 3. In *NASA Conference Proceedings 'Spacelab 3 Mission Science Review,' CP-2429* (ed. G. H. Fichtl), pp. 42–62. NTIS.
Gille, J. C. & Russell, J. M. III 1984 *J. geophys. Res.* **89**(D4), 5125–5140.
Gray, L. J. & Pyle, J. A. 1986 *Q. Jl R. met. Soc.* **112**, 387–407.
Grose, W. L., Turner, R. E. & Nealy, J. E. 1985 Transport processes in the stratosphere: model simulations and comparisons with satellite data. In *Middle atmosphere program (MAP) handbook*, vol. 18, pp. 381–385.
Handler, P. 1984 *Geophys. Res. Lett.* **11**, 1121–1124.

PHILOSOPHICAL TRANSACTIONS OF THE ROYAL SOCIETY A MATHEMATICAL, PHYSICAL & ENGINEERING SCIENCES

Harries, J. E. 1976 *Rev. Geophys. Space Phys.* **14**, 565.
Heath, D., Krueger, A. J. & Park, H. 1978 The solar backscatter ultraviolet (SBUV) and total ozone mapping spectrometer (TOMS) experiment. In *The Nimbus 7 Users' Guide*, (ed. C. R. Madrid), pp. 175–211. Greenbelt, Maryland: NASA Goddard Space Flight Center.
Hood, L. L. 1986 *J. geophys. Res.* **91**, 5264.
Jones, R. L. & Pyle, J. A. 1984 *J. geophys. Res.* **89**, 5263–5279.
Jones, R. L., Pyle, J. A., Harries, J. E., Zavody, A. M., Russell, J. M. III & Gille, J. C. 1986 *Q. Jl R. met. Soc.* **112**, 1127–1143.
Keating, G. M., Nicholson, J. III, Brasseur, G., DeRudder, A., Schmailzl, U. & Pitts, M. 1986 *Nature Lond* **322**, 43–46.
Kent, G. S. & McCormick, M. P. 1984 *J. geophys. Res.* **89**, 5303–5314.
Kent, G. S., Trepte, C. R., Farrukh, U. O. & McCormick, M. P. 1985 *J. atmos. Sci.* **42**, 1536–1551.
Kley, D. E., Stone, J., Henderson, W. R., Drummond, J. W., Harrop, W. J., Schmeltekopf, A. T., Thompson, T. L. & Winkler, R. H. 1979 *J. atmos. Sci.* **36**, 2513–2534.
Krueger, A. J., Stolarski, R. S., Alpert, J. C., Heath, D. F. & Chandra, S. 1985 *Eos, Wash.* **66**, 838.
Labitzke, K., Naujokot, B. & McCormick, M. P. 1983 *Geophys. Res. Lett.* **10**, 24–26.
Lippens, C., Muller, C., Vercheval, J., Ackerman, M., Laurent, J., Lemaitre, M. P., Besson, J. & Girard, A. 1984 *Adv. Space Res.* **4**(6), 75–79.
Mankin, W. G. & Coffey, M. T. 1984 *Science, Wash.* **256**, 170–172.
McCormick, M. P. 1985 *SAGE aerosol measurements, volume I–February 21, 1979, to December 31, 1979*. NASA RP 1144.
McCormick, M. P., Hamill, P., Pepin, T. J., Chu, W. P., Swissler, T. J. & McMaster, L. R. 1979 *Bull. Am. met. Soc.* **60**, 1038–1046.
McCormick, M. P., Steele, H. M., Hamill, P., Chu, W. P. & Swissler, T. J. 1982 *J. atmos. Sci.* **39**, 1387–1397.
McCormick, M. P., Trepte, C. R. & Kent, G. S. 1983 *Geophys. Res. Lett.* **10**, 941–944.
McCormick, M. P., Swissler, T. J., Fuller, W. H., Hunt, W. H. & Osborn, M. T. 1984 *Geof. Int.* **23–2**, 187–221.
McElroy, M. B., Salawitch, R. S., Wofsy, S. C. & Logan, J. A. 1986 *Nature Lond.* **321**, 759–762.
McMaster, L. R. 1986 In *Proc. of 6th Conf. on Atm. Rad. of the Am. Met. Soc., Williamsburg, Virginia*. American Meteorological Society.
McPeters, R. D., Heath, D. J. & Bhartia, P. K. 1984 *J. geophys. Res.* **89**, 5199–5214.
NASA/World Meterological Organization 1986 *Atmospheric ozone: assessment of our understanding of the processes controlling its present distribution and change. WMO Report* no. 16, WMO Global Ozone Research and Monitoring Project, Geneva, Switzerland.
National Academy of Sciences 1984 *Causes and effects of changes in stratospheric ozone: update 1983*. Washington, D.C.: National Academy Press.
Noxon, J. F. 1979 *J. geophys. Res.* **84**, 7883–7888.
Park, J. H., Zander, R., Farmer, C. B., Rinsland, C. P., Russell, J. M. III, Norton, R. H. & Raper, O. F. 1986 *Geophys. Res. Lett.* **13**(8), 765–768.
Remsberg, E. E., Russell, J. M. III, Gordley, L. L., Gille, J. C. & Bailey, P. L. 1984 *J. atmos. Sci.* **41**(21), 2934–2945.
Rinsland, C. P., Zander, R., Farmer, C. B., Norton, R. H., Brown, L. R., Russell, J. M. III & Park, J. H. 1986*a* *Geophys. Res. Lett.* **13**(8), 761–764.
Rinsland, C. P., Zander, R., Brown, L. R., Farmer, C. B., Park, J. H. Norton, R. H., Russell, J. M. III & Raper, O. F. 1986*b* *Geophys. Res. Lett.* **13**(8), 769–772.
Roscoe, H. K. 1982 *Geophys. Res. Lett.* **9**, 901–902.
Russell, J. M. III 1984 *Adv. Space Res.* **4**(4), 107–116.
Russell, J. M. III 1987 *Adv. Space Res.* (In the press.)
Russell, J. M. III, Solomon, S., Gordley, L. L., Remsberg, E. E. & Callis, L. B. 1984 *J. geophys. Res.* **89**(C8), 7267–7275.
Russell, J. M. III, Solomon, S., McCormick, M. P., Miller, A. J., Barnett, J. J., Jones, R. L. & Rusch, D. W. 1986 *Middle Atmosphere Program (MAP) Handbook*, vol. 22.
Schoeberl, M. R., Krueger, A. J. & Newman, P. 1986 *Geophys. Res. Lett.* **13**(12), 1217–1220.
Solomon, S. & Garcia, R. R. 1983 *J. geophys. Res.* **88**(C9), 5497–5501.
Solomon, S., Garcia, R. R. & Stordal, F. 1985*a* *J. Geophys. Res.* **90**(D7), 12 981–12 989.
Solomon, S., Garcia, R. R., Olivero, J. J., Bevilacqua, R. M., Schwartz, P. R., Clancy, R. T. & Muhleman, D. O. 1985*b* *J. atmos. Sci.* **42**(10), 1072–1083.
Solomon, S., Garcia, R. R., Rowland, F. S. & Weubbles, D. J. 1986*a* *Nature, Lond.* **321**, 755–758.
Solomon, S., Kiehl, J. T., Garcia, R. R. & Grose, W. L. 1986*b* *J. atmos. Sci.* **43**(15), 1603–1617.
Toon, G. C., Farmer, C. B. & Norton, R. H. 1986 *Nature, Lond.* **319**, 570–571.
Tung, K., Ko, M. K., Rodriguez, J. M. & Sze, N. D. 1986 *Nature, Lond.* **322**, 811–813.
Zander, R., Rinsland, C. P., Farmer, C. B., Brown, L. R. & Norton, R. H. 1986 *Geophys. Res. Lett.* **13**(8), 757–760.

PHILOSOPHICAL TRANSACTIONS OF THE ROYAL SOCIETY A MATHEMATICAL, PHYSICAL & ENGINEERING SCIENCES

Discussion

D. G. Andrews. To what extent can the optical properties of aerosol be taken as a measure of mixing ratio, hence giving information on atmospheric transport?

J. M. Russell III. The measured aerosol extinction is proportional to the integrated mass over the aerosol-size distribution. Therefore, the ratio of aerosol extinction to molecular extinction is similar to a mixing ratio. This ratio should be a conserved quantity except for aerosol settling, which is a slow process. Consequently, the aerosol should be a good tracer for transport studies, especially after volcanic events when large quantities of aerosol are injected into the stratosphere at a single geographic location.

F. W. Taylor. Dr Russell mentioned measurements of nitrogen-dioxide depletion over the winter pole that he interpreted as being caused by the formation of dinitrogen pentoxide (N_2O_5), and an enhancement of nitric acid in the same region that may be caused by conversion of dinitrogen pentoxide. What, in the light of this, should be our expectations now for the amounts of N_2O_5 in the polar night?

J. M. Russell III. A reasonable value to expect for polar-night N_2O_5 mixing ratio based on gas-phase chemistry is of the order of several parts per billion by volume. However, the enhancement of polar-night HNO_3 may be caused by heterogeneous processes involving N_2O_5 that are poorly understood. If this is so, it would be difficult to make a very good estimate of the mixing ratio.

PHILOSOPHICAL TRANSACTIONS OF THE ROYAL SOCIETY A MATHEMATICAL, PHYSICAL & ENGINEERING SCIENCES